Negative Feedback from Integrins to Cadherins: A Micromechanical Study

Alia Al-Kilani,[†] Olivier de Freitas,[†] Sylvie Dufour,[‡] and François Gallet[†*]
[†]Laboratoire Matière et Systèmes Complexes, UMR CNRS 7057 Université Paris-Diderot, Paris, France; and [‡]Compartimentation et dynamique cellulaires, UMR CNRS 144 Institut Curie, Paris, France

ABSTRACT The coupling between cell-cell and cell-matrix adhesion systems is known to affect the stability of the adhesive status of cells, as well as tissue cohesion. In this work, we perform quantitative assays of integrin-cadherin cross talk in controlled and reproducible conditions. This is achieved by plating cells on microprinted fibronectin patterns of different sizes, and simulating the formation of an intercellular contact with a microbead coated with E-cadherin extracellular domains and brought to the cell membrane. Using an optical trap, we measure the average rigidity modulus of the E-cadherin bead-cell contact as a function of the contact incubation time and of the cell spreading area. For a given incubation time, this rigidity modulus decreases by three orders of magnitude as the cell-matrix contact area, A, increases from 100 to 700 μm^2. In a similar way, the dynamics of formation of the bead-cell contact gets slower as this area increases. This is clear evidence for a strong negative feedback from cell-fibronectin onto cell-cell adhesive contacts, for which we discuss some possible mechanisms.

INTRODUCTION

Among the various transmembrane receptors that mediate cellular adhesion, cadherins and integrins constitute two major classes, which are the essential constituents of cell-cell and cell-matrix adhesive contacts, respectively. Through adhesive processes, these molecules are involved in many important functions, like cell migration, division, differentiation, and apoptosis. Most of the time, they act as mechanosensitive receptors, able to detect changes in the mechanical environment of the cell and to activate appropriate signaling by transmitting information toward the inner cell body, along the cytoskeleton filaments. Specific functions, like morphogenesis and wound healing, require a coordinated dynamics between contacts of different types to maintain the cohesion of the tissue. Modifications of this equilibrium may sometimes lead to epithelial-mesenchymal transition or tissue disruption, referring to either normal development processes (embryogenesis) or pathological situations (metastatic properties). Consequently, a subtle regulation between cell-cell and cell-matrix contacts is expected to occur in tissues, implying that cadherins and integrins are able to interact via mechanical, physical, and/or biochemical pathways.

Indeed, the cross talk processes between these two classes of adhesive receptors may be supported by different mechanisms (1): for instance, the adhesive complexes may communicate through mechanical connections supported by the cytoskeleton (actin filaments, bundles and stress fibers, or microtubules). Alternatively, the control may be ensured by signaling molecules carrying information from one adhesive system to another. Regulation may also come from an integrated response to a global cellular process (epithelial-mesenchymal transition, differentiation).

In the literature, one can find a few examples of such cross talk between adhesive contacts. Indeed, several works report that the cell-cell adherence status is modified as a function of integrin engagement in the extracellular matrix (ECM) (2–8). However, this engagement may lead either to a weakening, or to a reinforcement of intercellular adhesions, depending on the cell type, the cadherin species, the experimental methods, and/or the interaction mechanism. For instance, it has been shown that the actomyosin contraction, related to the enhancement of cell-matrix adhesive contacts induced by HGF treatment, may cause mechanical disruption of cadherin-cadherin contacts and scattering of MDCK cells (4). In a similar way, the interactions of integrins with fibronectin (FN)-coated beads in bovine endothelial aortic cells lead to disruption of the vascular-endothelial (VE)-cadherin bonds (5).

Conversely, it has been shown that blocking FN-integrin binding in *Xenopus* embryos (6) or using the null mutation in the FN gene of zebrafish embryos (7) prevents the formation of cadherin adhesive links. Recently, for S180 cells transfected to express E-cadherin (Ecad), measurements of the separation force between a cell doublet have shown that a greater force is required for cells bound to FN- or vitronectin-coated beads than for cells not interacting with ECM proteins (9). Many other examples demonstrate that the engagement of integrins in ECM contacts impairs or, conversely, favors the formation of intercellular adhesion mediated by cadherins. A few works also report reciprocal interactions involving regulation of integrin functions by cadherins (10).

Most of these works provide evidence for interaction effects, through the qualitative observation of contact reinforcement or disruption. However, until now, very few mechanical studies had been carried out to probe the variations of contact rigidity as a function of the parameters relevant for the control of the interaction, such as the cell spreading

Submitted July 28, 2010, and accepted for publication June 1, 2011.

*Correspondence: francois.gallet@univ-paris-diderot.fr

Editor: Lewis H. Romer.

0006-3495/11/07/0336/9 $2.00

doi: 10.1016/j.bpj.2011.06.009

area, density of adhesive contacts, geometry of adhesive patterns, and dynamics of contact formation.

In this work, our purpose is precisely to perform quantitative assays of the integrin-cadherin interactions in controlled and reproducible conditions. We study how the strength and growth dynamics of intercellular adhesions, supported by cadherins, are modulated by the shape and extension of cell-matrix adhesion, supported by integrins. This is achieved by following the formation and mechanical rigidity of the contact between a cell and a microbead functionalized with E-cadherin-extracellular-domain to model intercellular adhesion, as a function of the spreading area of the cell on a FN stamp, simulating integrin-mediated adhesion. We use Ecad cells derived from S180 murine sarcoma cells stably transfected to express E-cadherin at their surface and to acquire intercellular adhesion properties (11). Various conditions of cell spreading are achieved by plating Ecad cells on patterns of controlled size (10–35 μm) microprinted with FN. The formation of a cell-cell contact is simulated by bringing a bead coated with EcadFC fragments (Ecad-bead) into contact with the cell membrane. The Ecadbead-cell contact is maintained for growth and maturation during a given incubation time, τ (from 30 s to 15 min). Then, its stiffness is probed by applying a force step on the bead with an optical trap and measuring the cell deformation. An apparent Young's modulus, E, of the contact is measured as a function of the incubation time, τ, and of the cell-FN patterned contact area, A.

The most striking features emerging from our measurements are that for a typical incubation time, $\tau = 5$ min, the average stiffness, E, of the Ecadbead-cell contact decreases by three orders of magnitude as the cell spreading area on the FN changes from $A \approx 100\ \mu m^2$ (almost spherical cells) to $A \approx 600\ \mu m^2$ (widely spread cells). By following the dynamics of Ecadbead-cell contact, our measurements show that the typical growth time of a cadherin-mediated contact is about 2 min for a small cell-FN contact area ($0 < A < 150\ \mu m^2$) but much larger than 15 min for a large one ($A > 300\ \mu m^2$). To rule out possible effects due to nonspecific adhesion, we have performed several control experiments: 1), EGTA tests show that the Ecadbead-cell adhesion is, as expected, supported by E-cadherins ; 2), for cells grown on polylysine (PLL) instead of FN, the bead-cell stiffness does not depend on the cell spreading area. Also, when replacing Ecad fragments with Arg-Gly-Asp (RGD) peptides, it can be seen that the dynamics of integrin-RGD contact formation is independent of cell spreading, demonstrating the existence of feedback from integrins to cadherins but not to other integrins.

Our data unambiguously show that for Ecad cells, spreading on FN prevents, or at least considerably slows, the formation of cadherin-mediated contacts. At the end of the article, we discuss some possible mechanisms leading to such negative cross talk between cell-cell and cell-FN adhesive contacts.

MATERIALS AND METHODS

Cell lines, cell culture, and EGTA treatment

Ecad cells are an S180 mouse sarcoma clone stably transfected to produce E-cadherin-green fluorescent protein (GFP) (11). These Ecad cells were maintained at 37°C and 5% CO_2 atmosphere in Dulbecco's modified Eagle's medium (DMEM) supplemented with 10% fetal bovine serum (PAA, Pasching, Austria) and 1% penicillin/streptomycin (PAA). Confluent cultures were routinely split after treatment with trypsin/EDTA (PAA) in phosphate-buffered saline (PBS), and cultured on glass slides stamped with a mixture of FN and Cy3-FN (prepared from the Cy3 monoreactive dye pack, PA23001, Amersham Biosciences, Uppsala, Sweden). During cell spreading, the amount of serum is reduced to 2% to reduce the amount of surrounding adhesion proteins while preserving the cell viability. Fig. 1, *a* and *b*, shows pictures of S180 cells spread on square FN patterns of sizes 15 μm and 25 μm, respectively. Alternatively, Ecad cells were cultured on glass slides precoated with Poly-L-Lysine (Sigma, St. Louis, MO). E-cadherin-mediated adhesion requires calcium. In control experiments, Ca^{2+} was removed by incubation with Dulbecco's modified Eagle's medium containing 4 mM EGTA and 1 mM MgCl2 at 37°C, during ~1 h before starting measurements (12).

Stamping of fibronectin patterns

To make polydimethylsiloxane (PDMS) stamps, we used the protocol described in previous studies (13,14). After fabrication, the PDMS stamp was inked at room temperature during 45 min in humidified atmosphere with a solution of FN (80 μg/ml) and FN-Cy3 (7 μg/ml) in PBS. After removing the solution of FN, the PDMS surface was dried and FN was stamped on a silanized glass slide for 5 min. To prevent adhesion outside the patterns, the glass slide was then exposed to a PLL-g-PEG solution (SuSOS, Dübendorf, Switzerland) (0.1 mg/10 mM HEPES) for 1 h at room temperature and subsequently rinsed for 2–3 h in PBS.

Microbead preparation

Following the protocol described in Lambert et al. (15), sulfate latex microbeads 3.6 μm in diameter (Invitrogen, Carlsbad, CA) were incubated overnight at 4°C with 5–10 μg of human anti-Fc γ antibody (ref 109-005-098, Jackson IR, West Grove, PA) in 1 ml of 0.1 M borate buffer, pH 8.5. Beads were rinsed in PBS, then saturated for 1 h at room temperature in PBS-1%BSA, and 20 μl of the suspension was incubated at room temperature for 1.5 h with 10 μg of Ecad-Fc (648-EC-100, R&D Systems, Minneapolis, MN). These Ecadbeads were rinsed again three times in PBS-1% BSA. For RGD beads, carboxylated silica beads (3.47 μm diameter; Bangs Laboratories, Fishers, IN) were coated with a polypeptide containing the Arg-Gly-Asp (RGD) sequence (PepTide 2000; Telios Pharmaceuticals, San Diego, CA), according to the manufacturer's procedure.

Optical trapping and force application

To manipulate the beads, we use a conventional optical trapping system, obtained by focusing an infrared Ytterbium fiber laser ($\lambda = 1050$ nm, $P_{max} = 10$W; IPG Photonics, Oxford, MA) through the immersion objective (100×, NA 1.30) of an inverted microscope (IX71, Olympus, Hamburg, Germany). Here, the trap is kept at a fixed position, and the application of force is controlled by fine displacements of the experimental chamber by means of a piezoelectric stage (P-780, Polytec PI, Karlsruhe, Germany). First, a free Ecadbead is seized with the trap, brought into contact with the cell membrane, and maintained there during an incubation time, τ. The contact location is chosen at the cell side to conveniently visualize the bead and the contact region (see Fig. 1, *d* and *e*). Then, the Ecadbead-cell

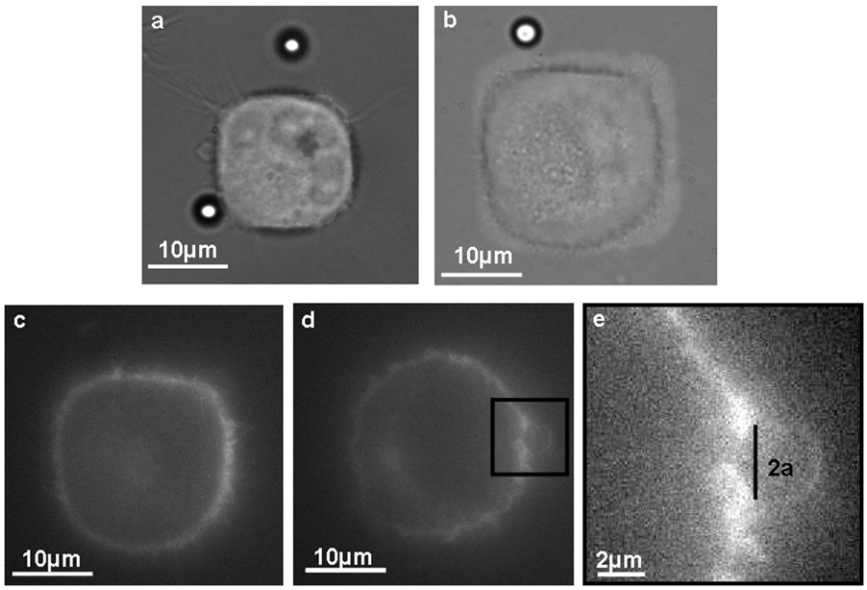

FIGURE 1 Pictures of Ecad-GFP cells spread on square FN-Cy3 patterns. (*a* and *b*) Cells on patterns of size 15 μm and 25 μm, respectively. (*c* and *d*) Fluorescence images of the cell in *b*, showing the cadherin-GFP distribution at the cell membrane. The images were taken at the basal plane (*c*), revealing the cell-pattern contact area, and at the height of the Ecadbead (*d*). (*e*) Enlarged view of the outlined segment of the cell in *d*, showing the contact zone between the cell and the Ecadbead, from which one can estimate the contact size, 2a.

contact is mechanically probed by applying a step of displacement to the piezoelectric stage (Fig. 2 *b*). The first forward step, which defines the initial time, $t = 0$, imprints a sharp displacement to both the cell and the bead attached to it. From that point, one follows the relaxation of the bead toward the trap center. The second step, which occurs at $t = 25$ s, brings the sample back to its initial position, inducing a backward relaxation of the bead, which is not considered in the following analysis. The force calibration was independently made by trapping a 3.6-μm latex bead in a counterflow of known velocity, v, and measuring its displacement, x_f, with respect to the trap center (16). The trapping force, F, is then equal to the Stokes' force. For small displacements, the force-displacement relationship is linear: $F = k \times x_f$, and the trap stiffness, k, is found to be proportional to the laser power. Applied forces are in the range 35–100 pN for an incident laser power $P = 0.4$ W.

Image recording and analysis

Numerical images were recorded from a high-sensitivity charge-coupled device camera (Coolsnap EZ, Roper Scientific, Trenton, NJ), through an ImageJ acquisition plugin. The bead position during its relaxation in the optical trap is tracked by a homemade ImageJ macro (acquisition rate of 50 Hz).

To precisely obtain the adhesive area between the cell and the FN pattern, we recorded simultaneous fluorescent images of the Cy3-FN pattern (Fig. 1 *b*) and the basal plane of the Ecad-GFP cell (Fig. 1 *c*) and measured the intersection area between the two.

To calculate the Young's modulus (see below), the diameter of the Ecadbead-cell contact area is required. This parameter can be estimated from a fluorescence image of Ecadherin-GFP at the bead-cell contact (Fig. 1 *e*).

Young's modulus calculation

From the recording of the relaxation of the bead position, $x_c(t)$, in response to a step of displacement, x_0, of the piezoelectric stage (see, for instance, the curve in Fig. 2 *b*), it is possible to retrieve all of the mechanical properties of the cell medium at the vicinity of the contact. Indeed, the force, F(t), exerted on the bead at time t after the step application is proportional to the bead-trap distance $x_f(t) = x_0 - x_c(t)$, and the bead displacement $x_c(t)$ is directly proportional to the cell deformation at the contact. However, it is well established that the intracellular medium comprising the cytoskeleton network, cannot be reduced to a simple elastic or Maxwell viscoelastic medium (17,18). For instance, it has been shown in numerous studies that the relationship between F(t) and $x_c(t)$ can only be properly represented by a delayed viscoelastic coefficient, exhibiting a weak power law with time (19). Therefore, measuring a Young's modulus could here appear as a vain exercise. Nevertheless, we decided to define an apparent Young's modulus, E, for the Ecadbead-cell contact response, since our goal here is to get a relative value to compare the contact stiffness for different adhesive conditions. More precisely, we define E here as the stress/strain ratio in the cell, both stress and strain being measured at the (arbitrary) time $t = 5$ s after the application of the step.

We assume that no deadhesion occurs during the traction assay of the bead (small deformation, duration <30 s), so that the bead-cell contact area remains constant during the mechanical test. The geometry of the contact is assumed to be a disk of radius a, measured by fluorescence microscopy as described in the previous paragraph. Then, the relationship between force F and displacement x_c is similar to the one provoked by the punch of an undeformable solid cylinder of diameter 2a into an elastic medium. This is a classical problem of linear elasticity, for which one finds (20)

$$x_c = \frac{1-\nu^2}{E}\frac{F}{2a}, \tag{1}$$

where E and ν are the Young's modulus and the Poisson's ratio, respectively, of the deformed medium. Assuming that the intracellular medium is incompressible ($\nu = 0.5$), one derives the equation that allows us to determine the apparent Young's modulus in the contact region:

$$E = \frac{3}{4}\frac{F}{2ax_c} \tag{2}$$

RESULTS

Ecad cells are cultivated for at least 3 h on FN micropatterns stamped on a glass coverslip. The different sizes of the square patterns are in the range 10–35 μm. To mimick the formation of an intercellular contact, an Ecadbead is trapped in an optical trap and brought into contact with a cell. After a given incubation time, τ (from 30 s to 15 min), the Ecadbead-cell contact rigidity is probed by applying a force on

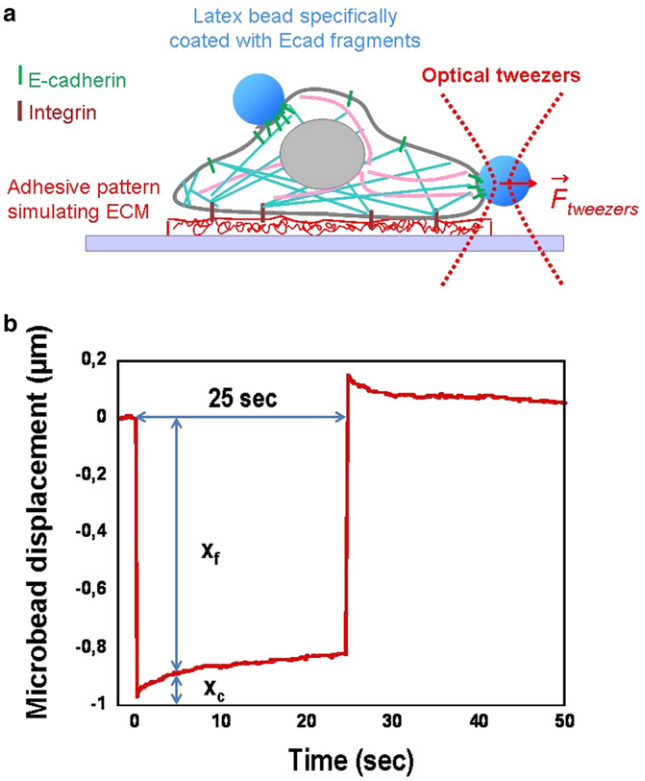

FIGURE 2 Scheme of the experimental protocol. (*a*) Ecad cells are grown on FN-stamped adhesive patterns of different sizes. Using an optical trap, an Ecadbead is brought into contact with the cell side. After an incubation time, τ, the Ecadbead-cell contact rigidity is probed by applying a force on the bead, through a back-and-forth step of displacement of the piezoelectric stage (see text). (*b*) After the first step, one records the relaxation of the bead toward the trap center ($0 < t < 25$ s). From the bead displacement, x_c, and the applied force (proportional to x_f), one calculates an apparent Young's modulus, E, of the contact 5 s after the step application.

the bead through a small step displacement (<1 μm) of the piezo stage (see Materials and Methods). The relaxation of the bead in the trap is recorded, and we retrieve an apparent Young's modulus, E, of the contact 5 s after the step application, according to Eq. 2. The displacements are small enough to remain in the small deformation regime.

The stiffness of Ecad-Ecad contact depends on FN-cell contact area

We measured the apparent Young's modulus of Ecadbead-cell contact under different conditions of incubation time, τ, and of spreading area, A. The measurement of E was not always possible, since a small percentage of beads did not adhere, or adhered only weakly, on the cells. This is the case when the bead completely relaxes in the trap immediately after the step force application, or when the contact disrupts before the 5-s waiting time arbitrarily chosen for E measurement. Actually, the percentage of nonadhering or weakly adhering beads varies from 17% to 1.5% when τ varies between 30 s and 10 min (Table 1).

Fig. 3 shows, on a logarithmic scale, the variations of Ecadbead-cell Young's modulus, E, measured after τ = 5 min incubation time, for 160 cells spread on FN patterns of different sizes. For each cell, the actual cell-FN contact area, A, is measured from the recorded image. Beads were attached to the cell either in the peripheral region, close to the basal surface (*red circles*) or in the central region, close to the nucleus (*blue diamonds*). In both cases, one notices a striking decrease of the contact rigidity, by three orders of magnitude from ~10^3 to 10^0 Pa, when the cell-FN spreading area, A, varies from ~100 μm^2 to 700 μm^2. This means that for cells weakly spread on the FN ($A < 100\ \mu m^2$) and almost spherical, a rigid intercellular contact develops after only 5 min incubation time. Conversely, for widely spread cells ($A > 400\ \mu m^2$), the Ecadbead-cell contact remains weak after the same incubation time. This observation does not depend on the location of the Ecadbead-cell contact, whether close to the basal surface or to the nucleus. Notice that we frequently observed a slow and centripetal motion of the bead, climbing up the cell toward the nucleus, especially when the bead-cell contact is tight. This behavior is similar to that reported in Lambert et al. (21) for NCad-coated beads attached to myogenic C2 cells.

Growth dynamics of the Ecadbead-cell contact

To probe the dynamics of contact formation, we measured the stiffness of the Ecadbead-cell contact after incubation times of 0.5, 1, 2, 5, 10, and >15 min. Fig. 4 shows the dependence of the apparent modulus, E, of bead-cell contact with incubation time τ, for three different classes of cell-FN contact area: 1), weakly spread cells ($A < 150\ \mu m^2$); 2), intermediate spreading ($150 < A < 300\ \mu m^2$); and 3), widely spread cells ($A > 300\ \mu m^2$). As could be expected, the rigidity of the Ecadbead-cell contact always increases when τ increases, but the dynamics is different according to the cell-FN spreading. When the spreading area, A, is <150 μm^2, the Young's modulus, E, increases rapidly with time before reaching a stable value around 450 Pa (there is no statistically significant difference between the average values of E measured at 2, 5, 10, and 15 min).

TABLE 1 Percentage of nonadhesive or weakly adhesive Ecadbead-cell contacts at different incubation times, τ

	30 s	1 min	2 min	5 min	10 min
−EGTA	17% (n = 29)	12% (n = 42)	11% (n = 36)	11% (n = 160)	1,5% (n = 36)
+EGTA	36% (n = 11)	30% (n = 11)	27% (n = 19)	23% (n = 19)	ND

Percentage of contacts under control conditions are shown in the top row, and those after EGTA addition in the bottom row. ND, not determined.

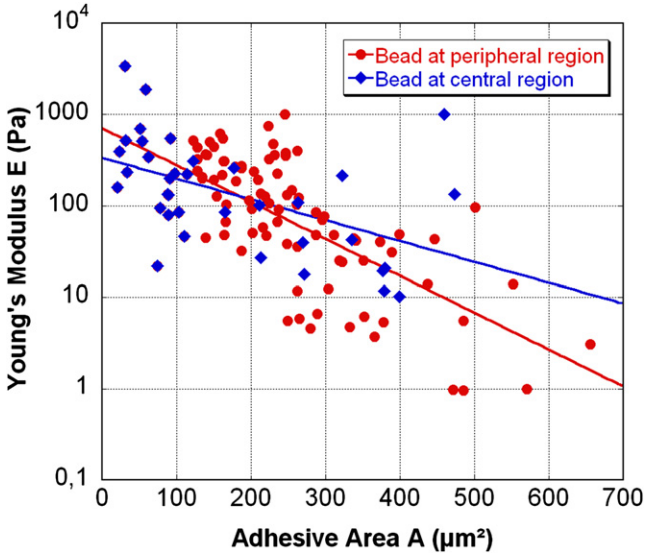

FIGURE 3 Plot of the apparent Young's modulus, E, of Ecadbead-cell contact versus cell spreading area on the FN pattern. E is measured after 5 min incubation time for the Ecadbead-cell contact, at two different locations of the cell: in the peripheral region (*circles*) or in the central region (*diamonds*). Solid lines, representing the best exponential fit through the data, are drawn as guides for the eye.

The time course necessary to reach this plateau value is ~2 min (Fig. 4). On the other hand, for intermediate spreading areas ($150 < A < 300\ \mu m^2$), the rigidity of the Ecadbead-cell contact continuously increases in the same time range ; it takes ~15 min to reach 450 Pa, a value similar to the plateau observed in the case of weakly spread cells. Finally, for widely spread cells ($A > 300\ \mu m^2$), no drastic change of E is observed up to $\tau = 10$ min, except for a slow increase of E with incubation time, an increase that may not be statistically significant. The contact stiffness remains small, of the order of 100 Pa, even for incubation times >15 min.

Taking advantage of the fact that E-cadherins are GFP-tagged in Ecad cells, we also tried to observe a redistribution of these receptors during contact formation. Unfortunately the GFP fluorescence level was quite strong everywhere at the cell membrane, so that no difference in cadherin density during contact formation could be detected. This may be caused by a low density of Ecad fragments on the beads. We were not able to measure this density, but it is expected to remain constant from one experiment to another. Staining other proteins like vinculin, or α- or β-catenin, would be an interesting alternative to observe the dynamics of recruitment of specific proteins at the intercellular contact (see Discussion).

Controls of Ecad-Ecad adhesion specificity

Homophilic adhesion of E-cadherin is known to be calcium-dependent. Therefore, to eliminate any potential artifacts due to cadherin-independent bead-cell interactions, an EGTA control has been performed to chelate extracellular Ca^{2+} and prevent E-cadherin-mediated adhesion. After incubating cells for 1 h with EGTA (4 mM) at 37°C, mechanical assays of Ecadbead-cell contact rigidity were performed as previously described, at different incubation times ($\tau = 0.5$, 1, 2, 5, and 10 min). As shown in Table 1, the percentage of nonadhering or weakly adhering Ecad-beads is substantially increased in the presence of EGTA, as compared to control conditions: this rate increases from 17% (− EGTA) to 36% (+ EGTA) at $\tau = 30$ s, and from 11%(− EGTA) to 23% (+ EGTA) at $\tau = 5$ min.

Fig. 5 shows a comparison of the average apparent Young's moduli of Ecadbead-cell contact with and without EGTA treatment. Here, cells with intermediate adhesion areas on an FN pattern ($150 < A < 300\ \mu m^2$) were selected, and different incubation times were tested. As compared to control conditions, which show an increase of E with

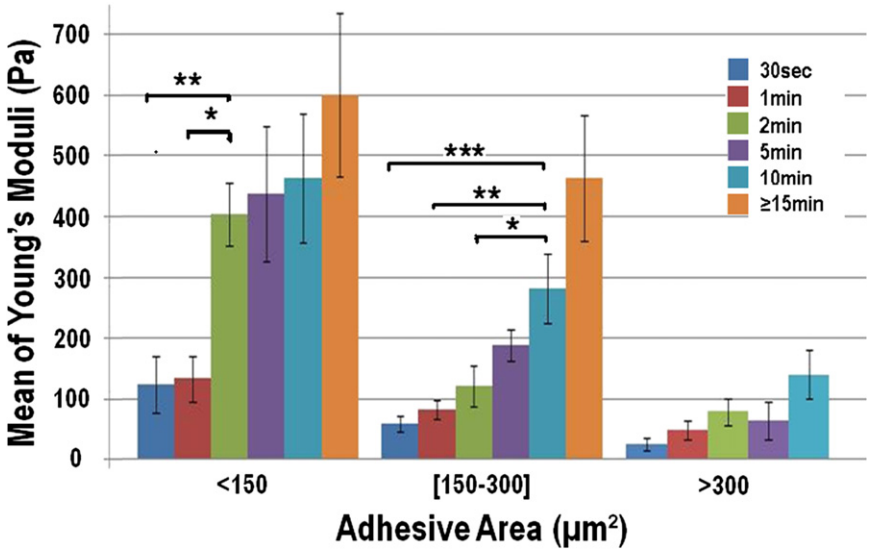

FIGURE 4 Evolution of the average Young's modulus, E, of Ecadbead-cell contact with incubation time, τ ($\tau = 0.5$, 1, 2, 5, 10, and >15 min). The rate of increase of the contact rigidity drastically depends on the cell-FN spreading area, A: for weakly spread cells ($A < 150\ \mu m^2$), E reaches a plateau value around 450 Pa in ~2 min; conversely, for widely spread cells, E increases very slowly and remains small (~100 Pa) even at $\tau = 10$ min. Error bars indicate the standard error; *p < 0.015; **p < 0.002 ; ***p < 0.001 (Student's *t*-test).

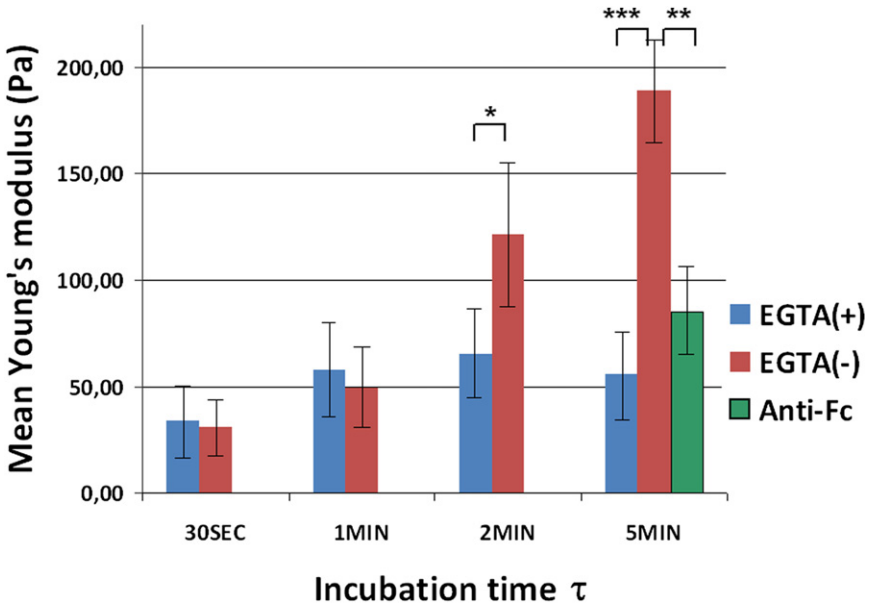

FIGURE 5 Effect of calcium-chelating EGTA on the average Young's modulus of Ecadbead-cell contact, for cells with intermediate adhesion areas on FN patterns ($150 < A < 300\ \mu m^2$). In control conditions (−EGTA), E increases with incubation time τ, whereas E remains constant at a low value, independent of τ, when EGTA is added. The averaged Young's modulus for beads carrying no Ecad fragments (anti-Fc beads) is also shown at $\tau = 5$ min ($150 < A < 300\ \mu m^2$). These controls demonstrate the specificity of Ecad-Ecad interactions in contact dynamics. Error bars indicate standard error; *p<0.08 ; **p<0.002; ***$p < 0.00002$ (Student's *t*-test).

incubation time, when EGTA is added, the apparent Young's modulus remains constant with time at ~50 Pa. This low-value apparent modulus is interpreted as due to remanent cadherin-independent adhesion (which, for convenience, we call nonspecific adhesion below). Since no contact strengthening is observed as time elapses in the presence of EGTA, we conclude that the increase of rigidity in standard conditions (in the presence of Ca^{2+}) is directly associated with homophilic E-cadherin-dependent contact development, as shown in Fig. 4.

We also note that even in the presence of EGTA, the level of cadherin-independent adhesion lies between 64% and 77%, when the incubating time τ varies from 30 s to 5 min (see Table 1). To determine the origin of this nonspecific adhesion, we repeated the experiment with the same latex beads carrying no Ecad fragments but coated with anti-Fc γ antibodies (anti-Fc beads). In this case, after 5 min incubation time, we observe a percentage of adhering beads of $61.5 \pm 7.5\%$ (four independent runs, $n = 91$ cells), as compared to $89 \pm 2.5\%$ (12 independent runs, $n = 160$ cells) for Ecad beads adhering to cells in standard conditions. The student's *t*-test between the two distributions leads to $p < 0.017$. Nonspecific adhesion (anti-Fc beads) is thus significantly lower than specific adhesion with Ecad-beads. Moreover, we measured the apparent Young's modulus, E, in such conditions (see Fig. 7). We found that E is on average lower with anti-Fc beads than with Ecad beads, and does not show any dependence on the cell's spreading area on FN ($n = 44$ cells). We conclude that a nonnegligible contribution of nonspecific adhesion superimposes to specific Ecad-Ecad adhesion to promote the binding of the bead to the cell surface. However, this nonspecific adhesion, probably due to the presence of other factors (perhaps proteins) on the bead surface, depends neither on incubation time, τ (Fig. 5), nor on cell spreading area, A, and thus can be clearly distinguished from specific adhesion. To further support this statement, we recall here the results of intercellular adhesion tests performed on both transfected and untransfected S180 cells (22,23). These assays have shown that nontransfected S180 cells (expressing no cadherins) present detectable, but weak and slowly developing, intercellular adhesion, whereas this adhesion rate is stronger and rises up more rapidly for cells transfected to express various cadherins (Ecad, Ncad, and cadherin-7).

Comparing FN adhesion with PLL adhesion

Previous results show that the rigidity and dynamics of an Ecadbead-cell contact mediated by cadherins is deeply affected by the adhesion area of the cell on an FN pattern. To assess the specific role of FN, and to rule out possible influences of adhesion geometry or cell morphology, we performed similar mechanical assays with cells spread on PLL-coated substrate. Fig. 6 shows the rigidity of Ecad-bead-cell contacts, measured after 5 min incubation time, for 25 cells cultivated on a PLL-coated glass slide and presenting different spreading areas (*blue diamonds*). These are compared with contacts measured under the same conditions for cells spread on FN patterns (*red circles*). Contrary to the large variation in E observed for cells on FN, E remains approximately constant for cells spread on PLL, in the range $10^2 - 10^3$ Pa over the full range $100 < A < 700\ \mu m^2$ (the slight decrease observed is not statistically significant). This demonstrates unambiguously that the variations of E reported in Figs. 3 and 4 are controlled by the engagement of integrins with FN in cell-matrix contacts, and not by the shape of the cell or by the spreading geometry on the substrate.

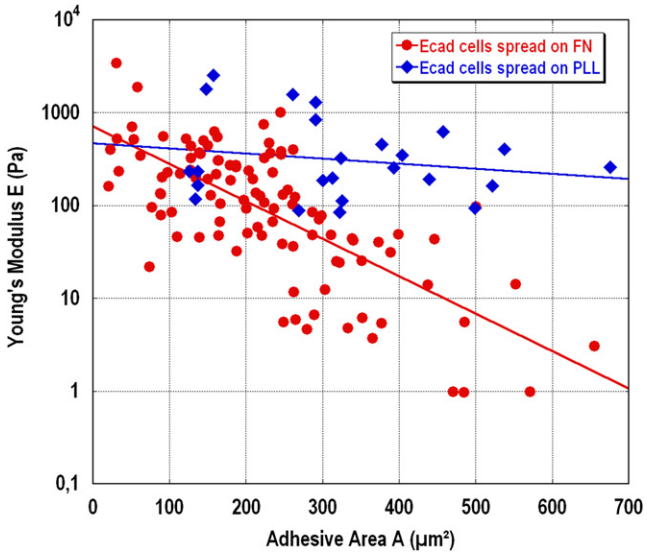

FIGURE 6 Comparison of the stiffness, E, of Ecadbead-cell contacts, for cells spread on a PLL-coated glass slide (*diamonds*) and for cells spread on FN patterns (*circles*). In the case of PLL substrate, no significant variation of E is observed when the spreading area varies from 100 to 700 μm^2.

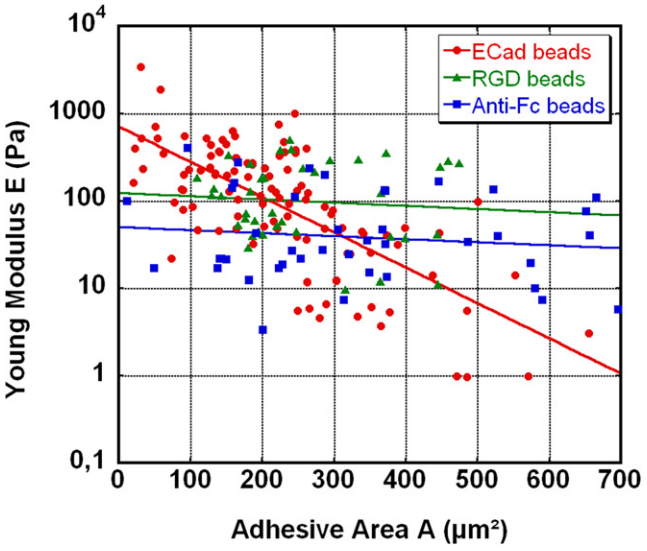

FIGURE 7 Comparison of the apparent stiffness E of Ecadbead-cell, anti-Fcbead-cell, and RGDbead-cell contacts, for cells spread on FN patterns of different areas, A (incubation time $\tau = 5$ min). Solid lines show the best exponential fits through the data, drawn as guides for the eye. Unlike the case of Ecadbeads, the apparent modulus, E, for beads coated only with anti-Fc ligands exhibits no dependence on A. This demonstrates that nonspecific adhesion is independent of cell spreading on FN. In a similar way, the rigidity of contacts made with RGDbeads is independent of A. Thus, the formation of a new integrin-mediated contact does not depend on the preexisting adhesive state of the cell to FN.

Contact formation to RGD-coated beads

To check whether the engagement of integrins to promote adhesion to FN could also influence the formation of new integrin-mediated contacts, we reproduced the experiment with beads coated by RGD peptide (RGDbeads) instead of Ecad fragments. RGD peptide is commonly used as a ligand to mimic integrin-FN binding. Using the same procedure described above, we measured the mechanical rigidity of the RGDbead-cell contact for 39 cells plated on FN patterns of different areas. Fig. 7 shows a comparison between the apparent moduli of Ecadbead-cell contacts and RGDbead-cell contacts, after 5 min incubation time, as a function of the spreading area, A, on FN patterns. Like anti-Fc beads, and contrary to Ecadbeads, the apparent modulus, E, for RGDbeads does not show any dependence on A. Thus, the formation of a new integrin-mediated contact does not depend on the state of cell adhesion to FN. This demonstrates that the negative feedback specifically occurs from integrins to cadherins, and not from integrins to integrins.

DISCUSSION

The objective of this work was to quantify the interactions between integrins and cadherins in a controlled environment in which the cell spreading area on FN is monitored by adhesive patterns, and the intercellular adhesion is mimicked by an Ecad-coated bead mechanically brought into contact with the cell membrane. This protocol provides reproducible conditions in which to assay the mechanical properties of a local intercellular contact mediated by cadherins, as a function of both incubation time and cell-FN adhesive area.

Two important results emerge from our experiments:

1. After allowing a given time for contact formation, the contact stiffness is measured with the help of optical tweezers. Stiffness drastically depends on the spreading area of the cell on the FN pattern: the more the cell is spread on the substrate, the weaker is the Ecadbead-cell contact. This effect is not dependent on the position of the contact at the cell membrane. On the other hand, it is directly related to the binding of integrins to proteins of the ECM (here FN). No such variation is observed when cells are plated on PLL. This unambiguously indicates that the engagement of the cell in adhesive contacts mediated by integrins has a very important negative effect on the formation of contacts mediated by cadherins.
2. The time required for the formation of an Ecadbead-cell contact also depends on the spreading of the cell on FN. Considering that the Ecad contact is fully developed when the apparent Young's modulus of Ecad adhesion has reached a plateau value of ~450 Pa, the characteristic timescale for bead-cell contact formation is of the order of 2 min for spherical cells weakly adherent to FN (Fig. 4). This time grows up to 15 min for cells with intermediate spreading area ($150 < A < 300$ μm^2), and is no longer measurable in the duration of our experiment for completely spread cells ($A > 300$ μm^2). The growth

dynamics of intercellular contact is thus considerably affected by preexisting adhesive contacts developed on FN. Conversely, the apparent rigidity of a newly formed integrin-RGD contact is not sensitive to the cell adhesive area on FN.

These results strongly support the theory of a negative feedback effect in Ecad cells from contacts mediated by integrins to those mediated by cadherins. Of course, they must be compared to other similar works, especially on S180 cells. Several articles have reported evidence for a cross talk between cadherins and integrins, either positive or negative, depending on cell line and experimental conditions (see Introduction). Actually, a recent study on the same S180 cell line apparently led to statements contradictory to ours (9): in that experiment, the force needed to separate two Ecad cells placed into contact for 4 min is measured by means of a dual pipette assay. The separation force increases when the cells have been incubated beforehand with FN-coated beads for 1 h. In this case, the feedback between integrins and cadherins appears to be positive, opposite to our own findings. However, the two experiments were performed in different conditions, and they do not probe the same properties. In the dual pipette assay, one measures the force needed to separate a cell doublet, either made from two cells suspended in the liquid medium, or prepared in an adhesive state on a 15-μm-diameter sphere coated with FN or PLL. In our experiment, the cell is not in suspension; it always presents adhesive contacts to a planar surface coated with FN, and we measure rigidity variations at the contact site between a cell and an Ecadbead as the adhesive FN-cell area is modified. In the first case, the force is in the nanonewton range, and is enough to disrupt the adhesive links, whereas in the second case, one uses much smaller stresses to probe the local rigidity. Also, the area of cell adhesion to the FN substrate is different in the two experiments. It is either null or remains small (~200 μm^2) in the dual pipette assay; it spreads on a larger range, from 100 to 700 μm^2, in the tweezers experiment. Finally, the cell morphology is different, since it remains mostly spherical in the first case, whereas it changes from a rounded to a completely spread shape in the second.

Another possible explanation lies in the different conditions of cadherin-cadherin interactions in the two experiments: the cell-cell contact area in the doublet is much larger than the bead-cell contact area in the model system. Moreover, the cadherins are free to diffuse along the cell membranes, allowing easier contact maturation than on a bead, where receptor diffusion is restricted. It is possible that the bead-cell experiment probes the earliest stages of the formation of a cadherin-cadherin contact and is less sensitive to the conditions of maturation of the contact, which require clustering of the adhesive receptors.

We therefore conclude that both the spreading conditions on FN and the intercellular adhesive status are not the same in the two experiments, which might explain the apparent discrepancy in the respective results.

At this point, the question arises about the origin of and possible mechanisms responsible for interactions between adhesive contacts of different nature. Several tracks have been proposed in the literature (see Introduction), and we can here formulate two hypotheses. First, the existence of internal mechanical stresses may be partly responsible for the nonassembly of intercellular adhesive complexes. Indeed, in a cell developing extended focal adhesions to the ECM, many actin filaments are associated in large bundles and stress fibers, and are kept under tension by myosin molecular motors. Active forces, constantly pulling on actin filaments from the basal plane, may prevent or delay the formation of adhesive complexes requiring the remodeling of actin filaments elsewhere in the cell, and especially at cell-cell contact areas. Another possible explanation is a biochemical regulation between cell-cell and cell-matrix contacts, ensured by some specific signaling. This signaling may involve kinases shared by different adhesive contacts, proteins directly or indirectly engaged at those sites, or changes in long-range membrane-cortex interactions.

To decide between these possibilities, our plan is to use appropriate staining to follow the remodeling of actin cytoskeleton during contact growth and observe the redistribution of specific proteins participating in intercellular contacts (for instance, vinculin, or α- or β-catenin). Inhibiting the actin cytoskeleton contractility would also bring information about a possible mechanical signaling between contacts of different natures.

To conclude, we have shown in this article that the mechanical properties and growth dynamics of an adhesive contact based on homophilic cadherin-mediated interactions are largely dependent on the preexisting status of cell adhesion on FN. We were able to quantify these interactions in a controlled experimental system, where the cell-ECM spreading area is governed by microprinted patterns of FN, and where an intercellular contact is mimicked by one bead coated with E-cadherin extracellular domain, and manipulated by optical tweezers. We observe a tight correlation between a large spreading of the cell on the substrate and a weak and slowly developing bead-cell adhesion. This is a clear signature for the existence of a strong negative feedback effect from cell-FN onto cell-cell adhesive contacts, for which we suggest some possible mechanisms.

We thank B. Ladoux for his help in stamping protocols, O. Cardoso for his help in image tracking software, L. Réa for workshop assistance, and A. Richert for cell cultures. J. P. Henry, B. Ladoux, and A. Asnacios are also acknowledged for fruitful discussions.

This work was supported by grants from the Agence Nationale de la Recherche, Physique et Chimie du Vivant (CrossInteCad 2007), and from the Association pour la Recherche sur le Cancer (subvention libre No. 3115).

REFERENCES

1. Chen, X., and B. M. Gumbiner. 2006. Crosstalk between different adhesion molecules. *Curr. Opin. Cell Biol.* 18:572–578.
2. Yano, H., Y. Mazaki, …, H. Sabe. 2004. Roles played by a subset of integrin signaling molecules in cadherin-based cell-cell adhesion. *J. Cell Biol.* 166:283–295.
3. Genda, T., M. Sakamoto, …, S. Hirohashi. 2000. Loss of cell-cell contact is induced by integrin-mediated cell-substratum adhesion in highly-motile and highly-metastatic hepatocellular carcinoma cells. *Lab. Invest.* 80:387–394.
4. de Rooij, J., A. Kerstens, …, C. M. Waterman-Storer. 2005. Integrin-dependent actomyosin contraction regulates epithelial cell scattering. *J. Cell Biol.* 171:153–164.
5. Wang, Y. X., G. Jin, …, S. Chien. 2006. Integrins regulate VE-cadherin and catenins: dependence of this regulation on Src, but not on Ras. *Proc. Natl. Acad. Sci. USA.* 103:1774–1779.
6. Marsden, M., and D. W. DeSimone. 2003. Integrin-ECM interactions regulate cadherin-dependent cell adhesion and are required for convergent extension in *Xenopus*. *Curr. Biol.* 13:1182–1191.
7. Trinh, L. A., and D. Y. R. Stainier. 2004. Fibronectin regulates epithelial organization during myocardial migration in zebrafish. *Dev. Cell.* 6:371–382.
8. Tsai, J., and L. Kam. 2009. Rigidity-dependent cross talk between integrin and cadherin signaling. *Biophys. J.* 96:L39–L41.
9. Martinez-Rico, C., F. Pincet, …, S. Dufour. 2010. Integrins stimulate E-cadherin-mediated intercellular adhesion by regulating Src-kinase activation and actomyosin contractility. *J. Cell Sci.* 123:712–722.
10. Borghi, N., M. Lownde, …, W. J. Nelson. 2010. Regulation of cell motile behavior by crosstalk between cadherin- and integrin-mediated adhesions. *Proc. Natl. Acad. Sci.* 107:13324–13329.
11. Chu, Y. S., W. A. Thomas, …, S. Dufour. 2004. Force measurements in E-cadherin-mediated cell doublets reveal rapid adhesion strengthened by actin cytoskeleton remodeling through Rac and Cdc42. *J. Cell Biol.* 167:1183–1194.
12. Munshi, H. G., S. Ghosh, …, M. S. Stack. 2002. Proteinase suppression by E-cadherin-mediated cell-cell attachment in premalignant oral keratinocytes. *J. Biol. Chem.* 277:38159–38167.
13. Ganz, A., M. Lambert, …, B. Ladoux. 2006. Traction forces exerted through N-cadherin contacts. *Biol. Cell.* 98:721–730.
14. Fink, J., M. Théry, …, M. Piel. 2007. Comparative study and improvement of current cell micro-patterning techniques. *Lab Chip.* 7:672–680.
15. Lambert, M., F. Padilla, and R. M. Mège. 2000. Immobilized dimers of N-cadherin-Fc chimera mimic cadherin-mediated cell contact formation: contribution of both outside-in and inside-out signals. *J. Cell Sci.* 113:2207–2219.
16. Balland, M., A. Richert, and F. Gallet. 2005. The dissipative contribution of myosin II in the cytoskeleton dynamics of myoblasts. *Eur. Biophys. J.* 34:255–261.
17. Alcaraz, J., L. Buscemi, …, D. Navajas. 2003. Microrheology of human lung epithelial cells measured by atomic force microscopy. *Biophys. J.* 84:2071–2079.
18. Balland, M., N. Desprat, …, F. Gallet. 2006. Power laws in microrheology experiments on living cells: comparative analysis and modeling. *Phys. Rev. E.* 74:021911.
19. Desprat, N., A. Richert, …, A. Asnacios. 2005. Creep function of a single living cell. *Biophys. J.* 88:2224–2233.
20. Johnson, K. 1985. Contact Mechanics. Cambridge University Press, Cambridge, United Kingdom.
21. Lambert, M., D. Choquet, and R. M. Mège. 2002. Dynamics of ligand-induced, Rac1-dependent anchoring of cadherins to the actin cytoskeleton. *J. Cell Biol.* 157:469–479.
22. Friedlander, D. R., R. M. Mège, …, G. M. Edelman. 1989. Cell sorting-out is modulated by both the specificity and amount of different cell adhesion molecules (CAMs) expressed on cell surfaces. *Proc. Natl. Acad. Sci. USA.* 86:7043–7047.
23. Dufour, S., A. Beauvais-Jouneau, …, J. P. Thiery. 1999. Differential function of N-cadherin and cadherin-7 in the control of embryonic cell motility. *J. Cell Biol.* 146:501–516.